Article:

Ryan, David E., Andrea, Kori A., Race, James J. et al. (3 more authors) (2020) Amine-Borane Dehydropolymerization Using Rh-Based Precatalysts:Resting State, Chain Control, and Efficient Polymer Synthesis. ACS Catalysis. pp. 7443-7448. ISSN: 2155-5435

https://doi.org/10.1021/acscatal.0c02211

ACS Catalysis

pubs.acs.org/acscatalysis

Letter

Amine−Borane Dehydropolymerization Using Rh-Based Precatalysts: Resting State, Chain Control, and Efficient Polymer Synthesis

David E. Ryan, Kori A. Andrea, James J. Race, Timothy M. Boyd, Guy C. Lloyd-Jones, and Andrew S. Weller*

Cite This: *ACS Catal.* 2020, 10, 7443−7448

Read Online

ACCESS | Metrics & More | Article Recommendations | Supporting Information

ABSTRACT: A detailed study of $H_3B{\cdot}NMeH_2$ dehydropolymerization using the cationic precatalyst $[Rh(DPEphos)(H_2BNMe_3(CH_2)_2{}^tBu)][BAr^F{}_4]$ identifies the resting state as dimeric $[Rh(DPEphos)H_2]_2$ and boronium $[H_2B(NMeH_2)_2]^+$ as the chain-control agent. $[Rh(DPEphos)H_2]_2$ can be generated in situ from Rh(DPEphos)(benzyl) and catalyzes polyaminoborane formation $(H_2BNMeH)_n$ [M_n = 15 000 g mol^{-1}]. Closely related Rh(Xantphos)(benzyl) operates at 0.1 mol % to give a higher molecular weight polymer [M_n = 85 000 g mol^{-1}] on the gram scale with low residual [Rh], 81 ppm. This insight offers a mechanistic template for dehydropolymerization.

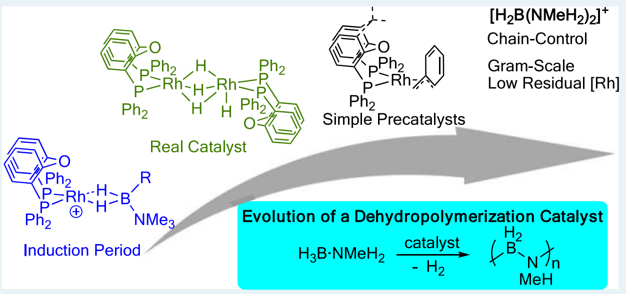

KEYWORDS: *dehydropolymerization, rhodium, phosphine, mechanism, amine−borane*

The catalyzed dehydropolymerization of amine−boranes, archetypically $H_3B{\cdot}NMeH_2$, is an atom-efficient methodology for the synthesis of polyaminoboranes $(H_2BNRH)_n$ (Scheme 1A), forming H_2 as the only byproduct.[1−4] This new class of main-group polymer[5] is based upon BN main-chain units and is isosteric with technologically mature polyolefins. These main-chain B−N units suggest, in addition to unexplored material and chemical properties, potential applications as piezoelectric materials[6,7] or as precursors to boron-based ceramics and *h*-BN.[1,8,9]

Scheme 1. (A) Amine−Borane Dehydropolymerization; (B) Exemplar Precatalyst Systems

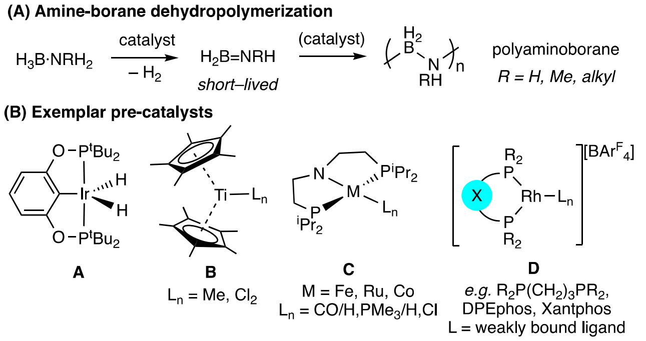

The currently accepted overarching mechanism for polymer formation from amine−borane involves initial dehydrogenation to form a transient[10] aminoborane ($H_2B{=}NRH$) that then undergoes end-chain nucleophilic B−N bond formation initiated by the catalyst.[3,11−16] While noncatalytic routes have been reported,[10,17] in terms of overall efficiency, scalability, substrate scope, and control of the polymer characteristics, catalytic routes offer the broadest opportunity for the tailored synthesis of polyaminoboranes.

A wide range of precatalyst systems have been described for amine−borane dehydropolymerization (Scheme 1B). After the original report of high[3] molecular weight polymer formed using $Ir(POCOP)H_2$ **A** [POCOP = κ^3-1,3-$({}^tBu_2PO)_2C_6H_3$],[1,11] systems based on group-4 metallocenes **B**,[18,19] cooperative ligands **C**,[14,16,20,21] and cationic $[RhL_2]^+$ precatalysts (L_2 = e.g., $Ph_2P(CH_2)_3PPh_2$, DPEphos, Xantphos) **D**[22−24] have been described. For the Rh-based catalysts, we have reported speciation, kinetics, and degree of polymerization studies. These are broadly generalized by an induction period, a nonliving chain-growth propagation, an inverse relationship between catalyst loading and degree of polymerization, and H_2 acting as a chain controlling agent to reduce polymer chain length,[15,22−24] Scheme 2.

Received: May 19, 2020
Revised: June 15, 2020
Published: June 17, 2020

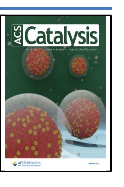

https://dx.doi.org/10.1021/acscatal.0c02211
ACS Catal. 2020, 10, 7443−7448

Scheme 2. Exemplar Complex 1 and Prior Observations

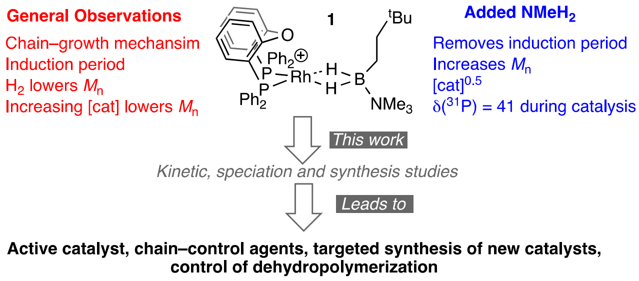

We have also reported on the key role of $NMeH_2$, formed by B−N bond cleavage in $H_3B{\cdot}NMeH_2$.[21,25] Exemplified using the $[Rh(DPEphos)(H_2BNMe_3CH_2CH_2{}^tBu)][BAr^F_4]$ precatalyst,[23] **1** [Ar^F = 3,5-$(CF_3)_2C_6H_3$], the amine $NMeH_2$ removes the induction period, increases the degree of polymerization, and simplifies the kinetics, allowing a half order dependency on $[Rh]_{TOTAL}$ to be determined. However, the structure of the active catalyst is undetermined, with insight limited to the detection of a single species at $\delta(^{31}P)$ 41.3 [J(RhP) = 150 Hz]. Also lacking is a robust explanation for the relationship between $[Rh]_{TOTAL}$ and H_2 on the degree of polymerization.

Despite these advances, the precise details of initiation, propagation, and termination remain to be determined for these diverse catalyst systems,[3] while the identification of resting states is rare[14,16] and challenging.[18] Herein, we report on an investigation of the $[Rh(DPEphos)]^+$ precatalyst system, **1**, in which a study of the kinetics, speciation, and synthesis has allowed the active catalyst to be identified, as well as the polymer-growth/termination processes to be interrogated. These insights are then harnessed in the design of a new, efficient, Rh-based catalyst that produces polyaminoborane on scale. A simple protocol is also described to significantly reduce the levels of residual catalyst in the isolated polymer.

We have previously reported that, when **1** is employed as precatalyst, the monocationic hydrido-aminoborane dimer $[Rh_2(DPEphos)_2(\mu\text{-}H)(\mu\text{-}H_2B{=}NHMe)][BAr^F_4]$ **2** is formed during the early stages of the reaction.[23] We propose this arises via an amine-promoted B−H hydride transfer[26] in a precursor cationic σ-amine−borane complex $[Rh(DPEphos)(H_3B{\cdot}NMeH_2)][BAr^F_4]$, **E**,[27] to generate a neutral hydride of empirical formula Rh(DPEphos)H (Scheme 3). Similar hydride species are formed in $[Rh(PONOP)(H_3B{\cdot}NMe_2H)]^+$[25] and $[Rh({}^iPr_2P(CH_2)_3P{}^iPr_2)(H_3B{\cdot}NH_3)]^+$[28] systems, alongside $H_2B{=}NMe_2/[NMe_2H_2]^+$ or boronium $[H_2B(NH_3)_2]^+$, respectively. On the basis of these observations, a simple kinetics model was constructed for the induction process, involving generation of **2** by rapid trapping of Rh(DPEphos)H with unreacted **E**, followed by a slow, amine-dependent, fragmentation to form the active catalyst. This telescopes the elementary steps of the induction process,[29] allows H_2 evolution to be used as proxy for transient $H_2B{=}NMeH$, and successfully reproduces the temporal concentration profiles,[23] as a function of $[Rh]_{TOTAL}$ (0.2 and 0.4 mol %) or when $NMeH_2$ is added, Scheme 3. A VTNA analysis[30,31] supports the observation of an empirical fractional order in the precatalyst: $[Rh]_{TOTAL}{}^{0.5}$.

Scheme 3. Model and Fitted Data[23 a]

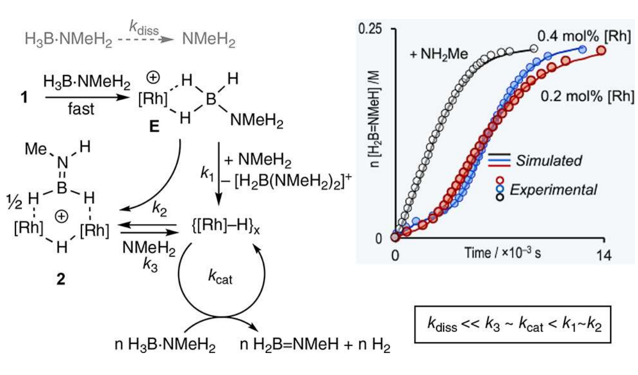

$^a[BAr^F_4]^-$ and DPEphos not shown. $[H_3B{\cdot}NMeH_2]$ = 0.223 M (1,2-$F_2C_6H_4$).

With an effective model for the induction process determined, we then focused on identification of the catalyst resting state. On the basis of our model and the work of Fryzuk et al.[32,33] and Han and Tilley,[34] the neutral hydride bridged dimer $[Rh(DPEphos)H_2]_2$, **3**, was synthesized in situ by the addition of either H_2 or $H_3B{\cdot}NMeH_2$ to the new benzyl complex Rh(κ^2-P,P-DPEphos)(η^3-H_2CPh) **4**, Scheme 4.

Scheme 4. Synthesis and Reactivity of Complex 3[a]

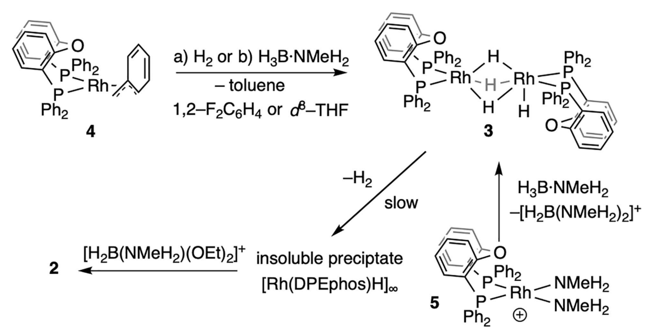

$^a[BAr^F_4]^-$ not shown.

Toluene is formed in all cases. The 298 K $^{31}P\{^1H\}$ NMR data for **3** match that observed during catalysis, i.e., δ 41.3 [J(RhP) = 150 Hz, THF-d_8]. The hydride ligands in **3** are fluxional at 298 K, presenting a very broad signal at δ −8.1. Cooling to 253 K reveals three environments at δ −6.9 (2H), −9.9 (1H), and −17.5 (1H). This pattern is similar to those reported for $Rh_2L_4H_4$ [L = P(O^{i}Pr)$_3$, 1/2 $^iPr_2P(CH_2)_3P^iPr_2$][32,35] and is indicative of three bridging hydrides and one terminal hydride. The $^{31}P\{^1H\}$ NMR spectrum of **3** at 253 K was poorly resolved, showing multiple, mutually coupled signals.

The addition of excess $H_3B{\cdot}NMeH_2$ to the amine complex $[Rh(DPEphos)(NMeH_2)_2][BAr^F_4]$, **5**,[23] also generates **3**, together with boronium $[H_2B(NMeH_2)_2]^+$ [$\delta(^{11}B)$ −7.8]. Solutions of complex **3** in 1,2-$F_2C_6H_4$, or in THF, irreversibly lose H_2 on degassing to form an insoluble yellow/brown powder, analyzed as $[Rh(DPEphos)H]_\infty$, likely to be a coordination polymer with Rh−H−Rh linkages. While the Rh-polymer does not dissolve on the addition of H_2, the soluble complex **2** is regenerated when $[H_2B(NMeH_2)(OEt_2)][BAr^F_4]$ is added.[10] Thus, when using a cationic precatalyst (i.e., **1** or **5**), persistent $NMeH_2$ will favor the soluble neutral hydride **3** via equilibration with complex **2** (k_3, Scheme 3). When using neutral precatalyst **4**, a high initial concentration of amine−borane, e.g., $[H_3B{\cdot}NMeH_2]_0$ = 0.446 M in THF, inhibits the formation of a precipitate. Presumably, the amine−borane intercepts Rh(DPEphos)H before it

https://dx.doi.org/10.1021/acscatal.0c02211
ACS Catal. 2020, 10, 7443−7448

oligomerizes. Thus, dimeric, neutral hydride **3** is observed as the common resting state, irrespective of the precatalyst or solvent. The half-order dependence in $[Rh]_{TOTAL}$ points to a rapid endergonic equilibrium between dimer and monomer, prior to the turnover limiting step. This has been noted in other Rh_2H_x systems,[32,36,37] and the data are thus consistent with the resting state being dimeric **3**. An important difference between neutral versus cationic precatalysts is that the latter generate a boronium coproduct, which has important implications for the dehydropolymerization, as discussed next.

Neutral precatalyst **4** was deployed in the dehydropolymerization of $H_3B{\cdot}NMeH_2$ at a variety of catalyst loadings, Table 1. Using 1,2-$F_2C_6H_4$ as the solvent, kinetics measurements

Table 1. GPC Characterization Data[a]

entry	cat.	$[Rh]_{TOTAL}$ (mol %)	M_n [M_p] (g mol^{-1})[b]	$Đ$	[boronium] (mol %)
1	**4**	0.25	15 000	2.5	0
2	**4**	0.5	15 000	2.5	0
3	**4**	1	15 000 [35 000]	2.4	0
4	**4**[c]	0.5	17 000	2.3	0
5	**4**[c]	1	17 000	2.4	0
6	**4**	1	[25 000]	n/a	0.25
7	**4**	1	[21 000]	n/a	0.5
8	**4**	1	[<19 000][d]	n/a	1
9	**6**	1	88 000	1.5	0
10	**6**	1	21 000	1.5	1
11	**6**[c,e]	0.1	85 000	1.5	0
13	**7**	1	98 000	1.6	0

[a]298 K, 1,2-$F_2C_6H_4$, 0.223 M $H_3B{\cdot}NMeH_2$, isobaric conditions under a flow of Ar; end point determined by ^{11}B NMR spectroscopy. [b]Relative to polystyrene standards; triple column; RI detection; THF with 0.1 w/w% $[NBu_4]Br$; 35 °C; [sample] = 2 mg cm^{-3}. [c]THF solvent. [d]M_p of the polymer distribution obscured by the $[BAr^F_4]^-$ signal. [e]5 M, 1.1 g scale.

were hampered by the formation of the insoluble precipitate. In THF, eudiometric measurements on H_2 production were less reliable due to solvent volatility. Nevertheless, polymerization goes to completion in both solvents, selectively forming $[H_2BNMeH]_n$, Figure 1A.[38] A plot of conversion versus M_n (Figure 1B, relative to polystyrene standards)[3,11,16] is characteristic of a nonliving chain-growth polymerization: at low conversions, the polymer is formed with high M_n and $H_3B{\cdot}NMeH_2$ dominates. Variations in catalyst loading did not affect the degree of polymerization of the resulting polyaminoborane, in either 1,2-$F_2C_6H_4$ (Figure 1C, M_n = 15 000 g mol^{-1}) or THF solutions (M_n = 17 000 g mol^{-1}), under "open conditions" with a slow Ar flow. This is different from cationic precatalysts, such as **1**, where M_n scales inversely with $[Rh]_{TOTAL}$: e.g., 6400 (1 mol %) and 34 900 g mol^{-1} (0.2 mol %).[23] However, "closed conditions" that allow for buildup of H_2 result in very low molecular weight oligomers being formed (1 mol % **4**, less than 1000 g mol^{-1} by GPC, ^{11}B NMR spectroscopy[31]). The cationic precatalyst **1** behaves analogously.[22]

The neutral and cationic precatalyst systems differ by the presence of a boronium coproduct with the latter, the relative concentration of which will scale with $[Rh]_{TOTAL}$.[39] Given the underlying insensitivity to the degree of polymerization to $[Rh]_{TOTAL}$ when using neutral **4**, we thus considered whether with cationic precatalysts boronium $[H_2B(NMeH_2)_2][BAr^F_4]$ can act as a chain-control agent to modify M_n. To test this,

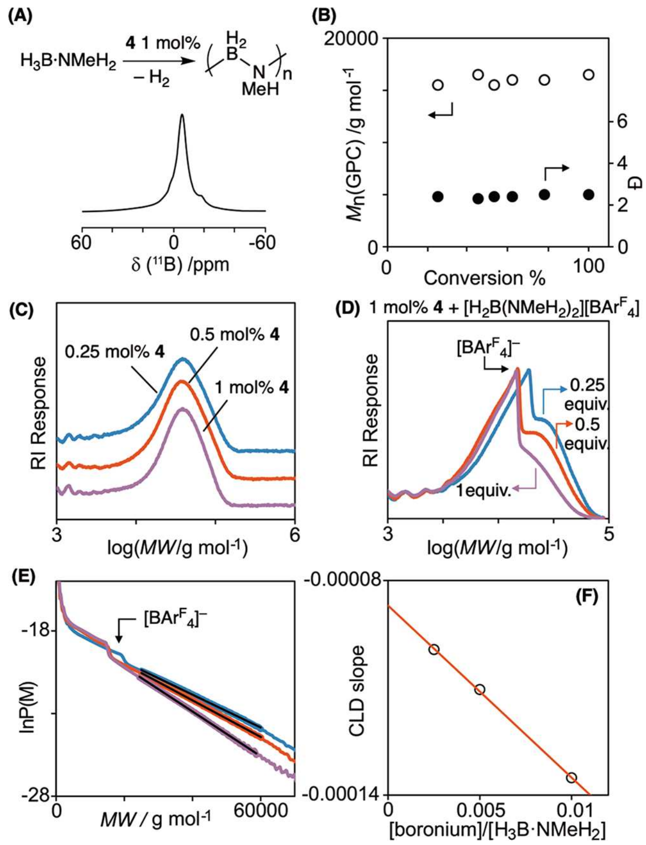

Figure 1. Polyaminoborane data obtained using catalyst **4** (Ar flow, 1,2-$F_2C_6H_4$, $H_3B{\cdot}NMeH_2$ = 0.223 M). (A) ^{11}B NMR spectrum of the polymer; (B) M_n versus conversion; (C) GPC data for 1.0, 0.5, and 0.25 mol % catalyst loadings; (D) GPC data for 1.0 mol % **4** with $[H_2B(NMeH_2)_2][BAr^F_4]$ doping; (E) ln–CLD plot of the high M_w fraction (D); (F) Mayo analysis.

$[H_2B(NMeH_2)_2][BAr^F_4]$ was doped (0.25 to 1 mol %) into 1 mol % **4**/$H_3B{\cdot}NMeH_2$ to selectively form polyaminoborane (^{11}B NMR). Although GPC analysis of the resulting polymer using refractive index detection is affected by the coeluting $[BAr^F_4]^-$ masking the lower molecular weight region (Figure 1D),[15] there is a qualitative trend of decreasing M_p with increasing $[H_2B(NMeH_2)_2][BAr^F_4]$, Table 1. This outcome is consistent with boronium acting as a chain-control agent. Chain length distribution (ln–CLD) analysis of high molecular weight fractions in GPC has been shown to be useful where there is overlap between distributions of polymer and transfer agents, such as that noted here, allowing for chain control processes to be probed.[40] A Mayo-type plot of [boronium]/$[H_3B{\cdot}NMeH_2]$ versus the ln–CLD slope indicates an inversely linear relationship (Figure 1E,F), further supporting the conclusion that the boronium functions as a rapid chain control agent in the dehydropolymerization.

Collectively, the analysis above facilitates the construction of a mechanistic landscape for dehydropolymerization, Scheme 5, that is consistent not only with the results herein but also with our previous observations on cationic Rh-based systems.[15,22,23,28,41] Thus, dehydrogenation of amine–borane to give the reactive monomer, $H_2B{=}NMeH$, occurs at a neutral [Rh–H] species in an H_2-mediated equilibrium with dimer **3**. Dehydrogenation to form $H_2B{=}NMeH$ via BH/NH activation (Scheme 5A) could be facilitated by a hemilabile DPEphos ligand (e.g., κ^2 and κ^3 coordination[42]) as previously

https://dx.doi.org/10.1021/acscatal.0c02211
ACS Catal. 2020, 10, 7443–7448

Scheme 5. Proposed (A) Catalyst Evolution/Dehydrogenation, (B) Propagation, and (C) Chain-Control Events

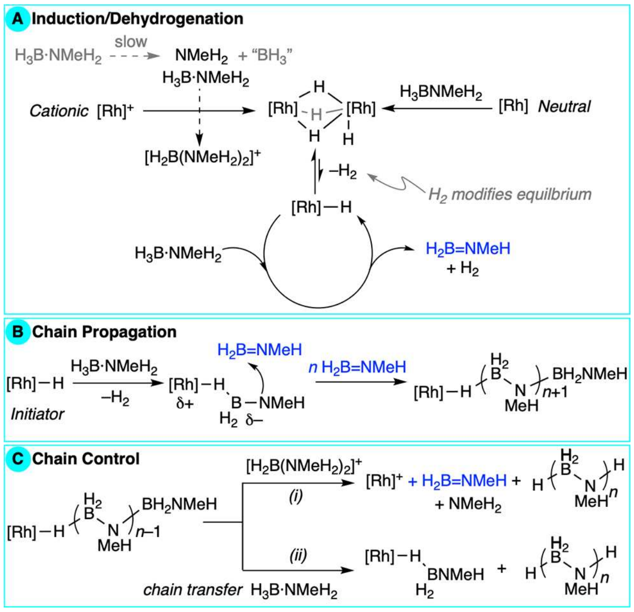

suggested.[43] Initiated by a formal hydride transfer from the rhodium hydride,[44] that is now playing a dual role in both dehydrogenation and initiation,[11,14] $H_2B{=}NMeH$ then undergoes rapid head-to-tail end-chain nucleophilic B–N bond formation, as proposed previously (Scheme 5B).[12,13,15,16] Chain control by protonation of the terminal nucleophilic amine of the polymeryl group by boronium returns a cationic precatalyst, aminoborane, and $NMeH_2$ that are rapidly recycled (Scheme 5C).[25] A related intramolecular proton transfer has been proposed by Paul and co-workers for Ir(POCOP)H_2 systems.[13] We speculate that, in the absence of boronium, chain transfer to premonomer $H_3B{\cdot}NMeH_2$ controls chain length, Scheme 5C. Whatever the precise mechanism for these chain-control processes, they result in relatively narrow dispersities of the final isolated polymer, as a result of the constant degrees of polymerization during the entire reaction (Figure 1B).[45] H_2 loss from **3**, and related systems,[32,35] occurs readily on degassing. The position of the initial monomer/dimer equilibrium is thus expected to be sensitive to [H_2], impacting the rate of dehydrogenation as well initiator concentration. This, we suggest, is the origin of the low degrees of polymerization observed under "closed conditions". In support of this, for a system where hydride-bridged dimer formation is disfavored due to sterics, e.g., Rh(Xantphos-^{i}Pr)H, H_2 does not act to modify the degree of polymerization.[15] The precise gearing of all of these interconnected relationships is therefore precatalyst, coproduct (e.g., boronium), and solvent specific.

The use of new precatalysts based upon neutral **4** demonstrates wider applicability and also signals the opportunity for the exploitation of structure/activity relationships (Figure 2, Table 1). For example, the Xantphos benzyl complex, **6**, is an effective precatalyst for dehydropolymerization (1 mol %, 88 000 g mol^{-1}, $Đ$ 1.6), and the degree of polymerization can be controlled by $[H_2B(NMeH_2)_2][BAr^F{}_4]$, e.g., 1 mol %, M_n = 21 000 g mol^{-1}. Complex **6** can be used at low loadings and high [$H_3B{\cdot}NMeH_2$] (0.1 mol %, 5 M in THF, using commercially sourced amine–borane) to produce high[3] molecular weight polyaminoborane on the gram scale (85 000 g mol^{-1}, 1.1 g). The use of activated charcoal in the polymer workup reduces the [Rh] content from 195 ppm (no workup) to 81 ppm. This is considerably lower than that reported for other Rh and Co-catalyzed dehydropolymerization systems.[15,21,46] The simple benzyl-dppp-catalyst **7** also promotes the formation of high molecular weight polyaminoborane (98 000 g mol^{-1}).

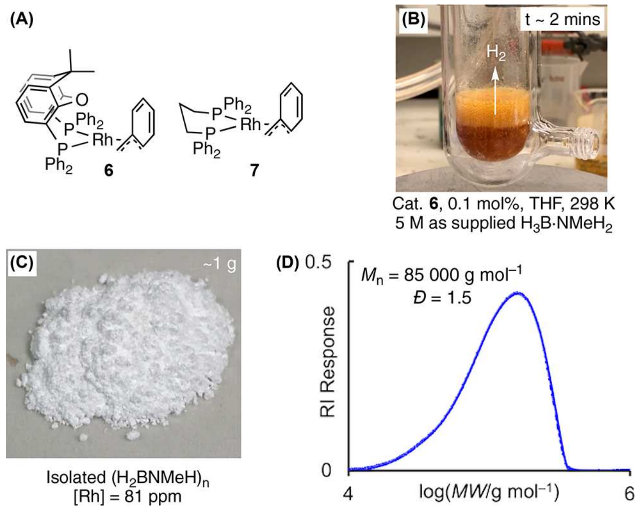

Figure 2. (A) New precatalysts. (B) Representative reaction. (C) Isolated polymer. (D) GPC trace [cat. = 5, 0.1 mol %].

In summary, the identification of the catalyst resting state, the events that lead to its formation, and thus the role that coproducts such as boronium and H_2 likely play in chain control have provided important insights into the complex and nuanced set of interconnected processes that are required for selective amine–borane dehydropolymerization using Rh-(bisphosphine)-based catalysts. While the detailed elucidation of the elementary steps awaits further study, Scheme 5 provides a testable framework for the analysis and design of catalyst systems for controlled amine–borane dehydropolymerization.

■ ASSOCIATED CONTENT

Supporting Information

The Supporting Information is available free of charge at https://pubs.acs.org/doi/10.1021/acscatal.0c02211.

Full experimental, structural, and kinetics data and details of the simulated model (PDF)

CIF files for complexes **4** and **6** (CIF)

■ AUTHOR INFORMATION

Corresponding Author

Andrew S. Weller – *Department of Chemistry, University of York, York YO10 5DD, United Kingdom;* orcid.org/0000-0003-1646-8081; Email: andrew.weller@york.ac.uk

Authors

David E. Ryan – *Department of Chemistry, University of York, York YO10 5DD, United Kingdom; Department of Chemistry, Chemical Research Laboratories, University of Oxford, Oxford OX1 3TA, United Kingdom;* orcid.org/0000-0001-8381-9502

Kori A. Andrea − *Department of Chemistry, Memorial University of Newfoundland, St. John's, Newfoundland A1B 3X7, Canada*

James J. Race − *Department of Chemistry, University of York, York YO10 5DD, United Kingdom; Department of Chemistry, Chemical Research Laboratories, University of Oxford, Oxford OX1 3TA, United Kingdom;* orcid.org/0000-0002-2134-3796

Timothy M. Boyd − *Department of Chemistry, University of York, York YO10 5DD, United Kingdom; Department of Chemistry, Chemical Research Laboratories, University of Oxford, Oxford OX1 3TA, United Kingdom;* orcid.org/0000-0001-6607-3761

Guy C. Lloyd-Jones − *School of Chemistry, University of Edinburgh, Edinburgh EH9 3FJ, United Kingdom;* orcid.org/0000-0003-2128-6864

Complete contact information is available at: https://pubs.acs.org/10.1021/acscatal.0c02211

Author Contributions

The manuscript was written through contributions of all authors.

Notes

The authors declare no competing financial interest.

■ ACKNOWLEDGMENTS

The authors acknowledge Drs. Romaeo Dallanegra and Adrian Chaplin for the synthesis and characterization of [Rh(κ^2-P,P-DPEphos)($\eta^2\eta^2$-$H_3B{\cdot}NMe_3$)][$BAr^F{}_4$] and Dr. Antonio Martinez-Martinez for useful discussions. EPSRC EP/M024210, the NSERC Vanier Canada Graduate Scholarship, and Michael Smith Foreign Study Supplement (KAA) are also acknowledged.

■ REFERENCES

(1) Staubitz, A.; Presa Soto, A.; Manners, I. Iridium-Catalyzed Dehydrocoupling of Primary Amine−Borane Adducts: A Route to High Molecular Weight Polyaminoboranes, Boron−Nitrogen Analogues of Polyolefins. *Angew. Chem., Int. Ed.* **2008**, *47*, 6212−6215.

(2) Leitao, E. M.; Jurca, T.; Manners, I. Catalysis in service of main group chemistry offers a versatile approach to p-block molecules and materials. *Nat. Chem.* **2013**, *5*, 817−829.

(3) Colebatch, A. L.; Weller, A. S. Amine−Borane Dehydropolymerization: Challenges and Opportunities. *Chem. - Eur. J.* **2019**, *25*, 1379−1390.

(4) Han, D.; Anke, F.; Trose, M.; Beweries, T. Recent advances in transition metal catalysed dehydropolymerisation of amine boranes and phosphine boranes. *Coord. Chem. Rev.* **2019**, *380*, 260−286.

(5) Vidal, F.; Jäkle, F. Functional Polymeric Materials Based on Main-Group Elements. *Angew. Chem., Int. Ed.* **2019**, *58*, 5846−5870.

(6) Nakhmanson, S. M.; Nardelli, M. B.; Bernholc, J. Ab Initio Studies of Polarization and Piezoelectricity in Vinylidene Fluoride and BN-Based Polymers. *Phys. Rev. Lett.* **2004**, *92*, 115504.

(7) Zhang, Y.; Hopkins, M. A.; Liptrot, D. J.; Khanbareh, H.; Groen, P.; Zhou, X.; Zhang, D.; Bao, Y.; Zhou, K.; Bowen, C. R.; Carbery, D. R. Harnessing Plasticity in an Amine-Borane as a Piezoelectric and Pyroelectric Flexible Film. *Angew. Chem., Int. Ed.* **2020**, *59*, 7808−7812.

(8) Du, V. A.; Jurca, T.; Whittell, G. R.; Manners, I. Aluminum borate nanowires from the pyrolysis of polyaminoborane precursors. *Dalton Trans.* **2016**, *45*, 1055−1062.

(9) Wang, X.; Hooper, T. N.; Kumar, A.; Priest, I. K.; Sheng, Y.; Samuels, T. O. M.; Wang, S.; Robertson, A. W.; Pacios, M.; Bhaskaran, H.; Weller, A. S.; Warner, J. H. Oligomeric aminoborane precursors for the chemical vapour deposition growth of few-layer hexagonal boron nitride. *CrystEngComm* **2017**, *19*, 285−294.

(10) Metters, O. J.; Chapman, A. M.; Robertson, A. P. M.; Woodall, C. H.; Gates, P. J.; Wass, D. F.; Manners, I. Generation of aminoborane monomers RR′N−BH_2 from amine−boronium cations [RR′NH−BH_2L]$^+$: metal catalyst-free formation of polyaminoboranes at ambient temperature. *Chem. Commun.* **2014**, *50*, 12146−12149.

(11) Staubitz, A.; Sloan, M. E.; Robertson, A. P. M.; Friedrich, A.; Schneider, S.; Gates, P. J.; Schmedt auf der Günne, J.; Manners, I. Catalytic Dehydrocoupling/Dehydrogenation of N-Methylamine-Borane and Ammonia-Borane: Synthesis and Characterization of High Molecular Weight Polyaminoboranes. *J. Am. Chem. Soc.* **2010**, *132*, 13332−13345.

(12) Baker, R. T.; Gordon, J. C.; Hamilton, C. W.; Henson, N. J.; Lin, P.-H.; Maguire, S.; Murugesu, M.; Scott, B. L.; Smythe, N. C. Iron Complex-Catalyzed Ammonia−Borane Dehydrogenation. A Potential Route toward B−N-Containing Polymer Motifs Using Earth-Abundant Metal Catalysts. *J. Am. Chem. Soc.* **2012**, *134*, 5598−5609.

(13) Bhunya, S.; Malakar, T.; Paul, A. Unfolding the crucial role of a nucleophile in Ziegler−Natta type Ir catalyzed polyaminoborane formation. *Chem. Commun.* **2014**, *50*, 5919−5922.

(14) Glüer, A.; Förster, M.; Celinski, V. R.; Schmedt auf der Günne, J.; Holthausen, M. C.; Schneider, S. Highly Active Iron Catalyst for Ammonia Borane Dehydrocoupling at Room Temperature. *ACS Catal.* **2015**, *5*, 7214−7217.

(15) Adams, G. M.; Colebatch, A. L.; Skornia, J. T.; McKay, A. I.; Johnson, H. C.; Lloyd-Jones, G. C.; Macgregor, S. A.; Beattie, N. A.; Weller, A. S. Dehydropolymerization of $H_3B{\cdot}NMeH_2$ To Form Polyaminoboranes Using [Rh(Xantphos-alkyl)] Catalysts. *J. Am. Chem. Soc.* **2018**, *140*, 1481−1495.

(16) Anke, F.; Boye, S.; Spannenberg, A.; Lederer, A.; Heller, D.; Beweries, T. Dehydropolymerisation of methylamine borane and an N-substituted primary amine borane using a PNP Fe catalyst. *Chem. - Eur. J.* **2020**, *26*, 7889−7899.

(17) De Albuquerque Pinheiro, C. A.; Roiland, C.; Jehan, P.; Alcaraz, G. Solventless and Metal-Free Synthesis of High-Molecular-Mass Polyaminoboranes from Diisopropylaminoborane and Primary Amines. *Angew. Chem., Int. Ed.* **2018**, *57*, 1519−1522.

(18) LaPierre, E. A.; Patrick, B. O.; Manners, I. Trivalent Titanocene Alkyls and Hydrides as Well-Defined, Highly Active, and Broad Scope Precatalysts for Dehydropolymerization of Amine-Boranes. *J. Am. Chem. Soc.* **2019**, *141*, 20009−20015.

(19) Jurca, T.; Dellermann, T.; Stubbs, N. E.; Resendiz-Lara, D. A.; Whittell, G. R.; Manners, I. Step-growth titanium-catalysed dehydropolymerisation of amine−boranes. *Chem. Sci.* **2018**, *9*, 3360−3366.

(20) Knitsch, R.; Han, D.; Anke, F.; Ibing, L.; Jiao, H.; Hansen, M. R.; Beweries, T. Fe(II) Hydride Complexes for the Homogeneous Dehydrocoupling of Hydrazine Borane: Catalytic Mechanism via DFT Calculations and Detailed Spectroscopic Characterization. *Organometallics* **2019**, *38*, 2714−2723.

(21) Boyd, T. M.; Andrea, K. A.; Baston, K.; Johnson, A.; Ryan, D. E.; Weller, A. S. A simple cobalt-based catalyst system for the controlled dehydropolymerisation of $H_3B{\cdot}NMeH_2$ on the gram-scale. *Chem. Commun.* **2020**, *56*, 482−485.

(22) Johnson, H. C.; Leitao, E. M.; Whittell, G. R.; Manners, I.; Lloyd-Jones, G. C.; Weller, A. S. Mechanistic Studies of the Dehydrocoupling and Dehydropolymerization of Amine−Boranes Using a [Rh(Xantphos)]$^+$ Catalyst. *J. Am. Chem. Soc.* **2014**, *136*, 9078−9093.

(23) Adams, G. M.; Ryan, D. E.; Beattie, N. A.; McKay, A. I.; Lloyd-Jones, G. C.; Weller, A. S. Dehydropolymerization of $H_3B{\cdot}NMeH_2$ Using a [Rh(DPEphos)]$^+$ Catalyst: The Promoting Effect of $NMeH_2$. *ACS Catal.* **2019**, *9*, 3657−3666.

(24) Colebatch, A. L.; Hawkey Gilder, B. W.; Whittell, G. R.; Oldroyd, N. L.; Manners, I.; Weller, A. S. A General, Rhodium-Catalyzed, Synthesis of Deuterated Boranes and N-Methyl Polyaminoboranes. *Chem. - Eur. J.* **2018**, *24*, 5450−5455.

(25) Spearing-Ewyn, E. A. K.; Beattie, N. A.; Colebatch, A. L.; Martinez-Martinez, A. J.; Docker, A.; Boyd, T. M.; Baillie, G.; Reed, R.; Macgregor, S. A.; Weller, A. S. The role of neutral Rh(PONOP)H, free NMe_2H, boronium and ammonium salts in the dehydrocoupling of dimethylamine-borane using the cationic pincer $[Rh(PONOP)(\eta^2\text{-}H_2)]^+$ catalyst. *Dalton Trans.* **2019**, *48*, 14724−14736.
(26) Roselló-Merino, M.; López-Serrano, J.; Conejero, S. Dehydrocoupling Reactions of Dimethylamine-Borane by Pt(II) Complexes: A New Mechanism Involving Deprotonation of Boronium Cations. *J. Am. Chem. Soc.* **2013**, *135*, 10910−10913.
(27) See the Supporting Information for the model complex for **E**: $[Rh(\kappa^2\text{-P,P-DPEphos})(\eta^2\eta^2\text{-}H_3B\cdot NMe_3)][BAr^F_4]$.
(28) Kumar, A.; Beattie, N. A.; Pike, S. D.; Macgregor, S. A.; Weller, A. S. The Simplest Amino-borane $H_2B = NH_2$ Trapped on a Rhodium Dimer: Pre-Catalysts for Amine−Borane Dehydropolymerization. *Angew. Chem., Int. Ed.* **2016**, *55*, 6651−6656.
(29) These will be defined and discussed in a future contribution.
(30) Nielsen, C. D. T.; Burés, J. Visual kinetic analysis. *Chem. Sci.* **2019**, *10*, 348−353.
(31) See the Supporting Information.
(32) Fryzuk, M. D.; Piers, W. E.; Einstein, F. W. B.; Jones, T. Coordinatively unsaturated binuclear clusters of rhodium. The reactivity of $[\{Pr^i_2P(CH_2)_nPPr^i_2\}Rh]_2(\mu\text{-}H)_2$ (n = 2, 3, and 4) with dihydrogen, and their use in the catalytic hydrogenation of olefins. *Can. J. Chem.* **1989**, *67*, 883−896.
(33) Fryzuk, M. D.; McConville, D. H.; Rettig, S. J. Synthesis, structure and hydrogenation of η^3-benzyl diphosphine complexes of rhodium and iridium. *J. Organomet. Chem.* **1993**, *445*, 245−256.
(34) Han, L.-B.; Tilley, T. D. Selective Homo- and Heterodehydrocouplings of Phosphines Catalyzed by Rhodium Phosphido Complexes. *J. Am. Chem. Soc.* **2006**, *128*, 13698−13699.
(35) Sivak, A. J.; Muetterties, E. L. Metal clusters. 21. Synthesis of rhodium phosphite clusters. *J. Am. Chem. Soc.* **1979**, *101*, 4878−4887.
(36) Kumar, A.; Ishibashi, J. S. A.; Hooper, T. N.; Mikulas, T. C.; Dixon, D. A.; Liu, S.-Y.; Weller, A. S. The Synthesis, Characterization and Dehydrogenation of Sigma-Complexes of BN-Cyclohexanes. *Chem. - Eur. J.* **2016**, *22*, 310−322.
(37) Brown, J. M.; Lloyd-Jones, G. C. Vinylborane Formation in Rhodium-Catalyzed Hydroboration of Vinylarenes. Mechanism versus Borane Structure and Relationship to Silation. *J. Am. Chem. Soc.* **1994**, *116*, 866−878.
(38) Monitoring by NMR spectroscopy (1 mol %, THF, closed system) shows no induction period.
(39) Some neutral precatalyst systems may also produce coproducts that scale with [cat], such as boronium or ammonium, through amine-promoted M−Cl for M−H metathesis. See ref 21.
(40) Moad, G.; Moad, C. L. Use of Chain Length Distributions in Determining Chain Transfer Constants and Termination Mechanisms. *Macromolecules* **1996**, *29*, 7727−7733.
(41) Dallanegra, R.; Robertson, A. P. M.; Chaplin, A. B.; Manners, I.; Weller, A. S. *Chem. Commun.* **2011**, *47*, 3763.
(42) Adams, G. M.; Weller, A. S. POP-type ligands: Variable coordination and hemilabile behaviour. *Coord. Chem. Rev.* **2018**, *355*, 150−172.
(43) Esteruelas, M. A.; Nolis, P.; Oliván, M.; Oñate, E.; Vallribera, A.; Vélez, A. Ammonia Borane Dehydrogenation Promoted by a Pincer-Square-Planar Rhodium(I) Monohydride: A Stepwise Hydrogen Transfer from the Substrate to the Catalyst. *Inorg. Chem.* **2016**, *55*, 7176−7181.
(44) Addy, D. A.; Bates, J. I.; Kelly, M. J.; Riddlestone, I. M.; Aldridge, S. Aminoborane σ Complexes: Significance of Hydride Co-ligands in Dynamic Processes and Dehydrogenative Borylene Formation. *Organometallics* **2013**, *32*, 1583−1586.
(45) Chain-capping events have been discussed in phospine−borane dehydropolymerization. Oldroyd, N. L.; Chitnis, S. S.; Annibale, V. T.; Arz, M. I.; Sparkes, H. A.; Manners, I. Metal-free dehydropolymerisation of phosphine-boranes using cyclic (alkyl)(amino)carbenes as hydrogen acceptors. *Nat. Commun.* **2019**, *10*, 1370.
(46) Turner, J. R.; Resendiz-Lara, D. A.; Jurca, T.; Schäfer, A.; Vance, J. R.; Beckett, L.; Whittell, G. R.; Musgrave, R. A.; Sparkes, H. A.; Manners, I. Synthesis, Characterization, and Properties of Poly(aryl)phosphinoboranes Formed via Iron-Catalyzed Dehydropolymerization. *Macromol. Chem. Phys.* **2017**, *218*, 1700120.

NOTE ADDED AFTER ASAP PUBLICATION

This paper was originally published ASAP on June 24, 2020, with an error in Scheme 4. The corrected version was reposted on June 29, 2020.

https://dx.doi.org/10.1021/acscatal.0c02211
ACS Catal. 2020, 10, 7443−7448